Article

Intermolecular Charge Transfer and Hydrogen Bonding in Solid Furan

Manuel Montejo, Amparo Navarro, Gordon J. Kearley, Juana Vzquez, and Juan Jess Lpez-Gonzlez

J. Am. Chem. Soc., **2004**, 126 (46), 15087-15095• DOI: 10.1021/ja040130y • Publication Date (Web): 29 October 2004

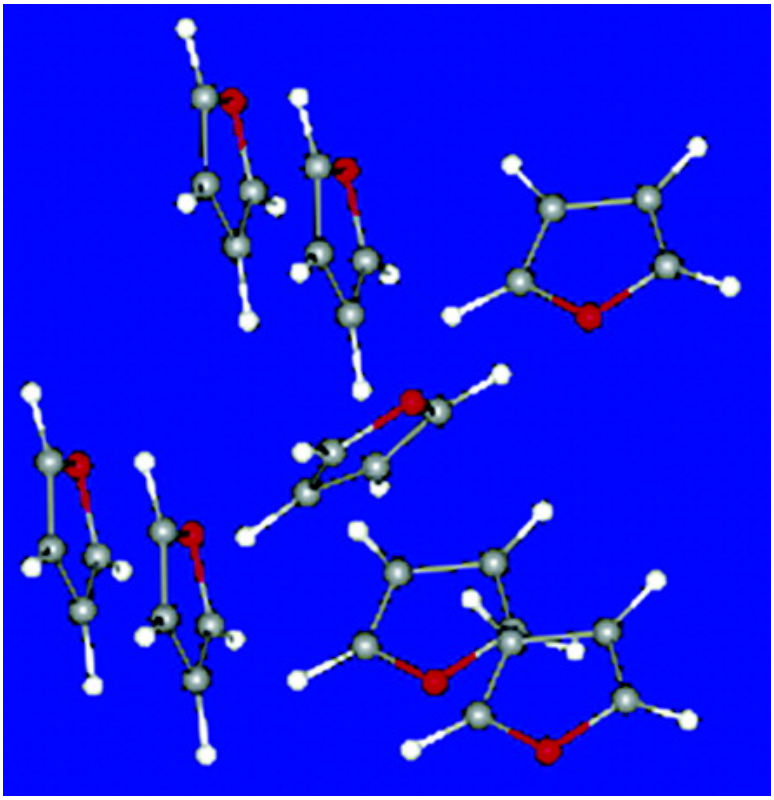

J|A|C|S
ARTICLES
Published on Web 10/29/2004

Intermolecular Charge Transfer and Hydrogen Bonding in Solid Furan

Manuel Montejo,[†] Amparo Navarro,*[,†] Gordon J. Kearley,[‡] Juana Vázquez,[†] and Juan Jesús López-González[†]

Contribution from the Department of Physical and Analytical Chemistry, University of Jaén, 23071 Jaén, Spain, and TU Delft, Interfacultair Reactor Institute, Mekelweg 15, 2629 JB Delft, The Netherlands

Received May 10, 2004; E-mail: anavarro@ujaen.es

Abstract: The calculated structures of furan as a monomer, a dimer that was isolated from the crystal structure, and the full crystal structure have been thoroughly investigated by a combination of density functional theory (DFT) calculations and inelastic neutron scattering (INS) measurements. To improve our understanding of the nature and magnitude of the intermolecular interactions in the solid, the atoms in molecules (AIM) theory has been applied to the dimer and a cluster of eight monomers. After a careful topological study of the theoretical charge density and of its Laplacian, we have established the existence of C−H···π, C−H···O, and H···H interactions between adjacent molecules in solid furan. The electron distribution has also been analyzed by performing natural bond orbital (NBO) calculations for the monomer and a H-bonded dimer. When the hydrogen bond is established between two adjacent furan rings, some electron charge is transferred from the π electronic system of one furan ring to the other molecule in the dimer. This result provides a model of the interaction between end groups of neighboring chains of polyfuran and could be applicable to other conjugated polymers where the π system is responsible for their conducting properties. To determine how the intermolecular bonds in the solid affect the vibrational dynamics in the periodic system, INS data were analyzed by performing molecular and periodic density functional calculations. Reasonable agreement is achieved, although we note that the poorest agreement is for modes involving hydrogen atoms.

1. Introduction

Five-membered aromatic heterocyclic molecules (furan, thiophene, and pyrrole) and their derivatives have been widely studied, from both a scientific and a technological point of view, during the last century because they often occur as a part of larger biomolecules[1] and macromolecules.[2] The furan ring is of key importance in biochemistry and biophysics since it can be found as a part or structural unit in a number of drugs and polymers, as well as in many biological molecules, such as chlorophyll, biotin, vitamin B-12, and so forth. It is also an important constituent in synfuel products that are of major interest in the coal conversion industry and is a precursor in several synthetic paths in organic chemistry.[3] More recently, the synthesis of furan copolymers from renewable vegetable resources (biomass), using simple chemical reactions, has found wide application in the paints industry, in which they are being used in place of petroleum-based copolymers.[2]

Nowadays, the development of conducting polymers represents a cross-disciplinary field of considerable interest.[4] These materials differ from conventional polymers because they possess a π system that is delocalized along the chain, providing a pathway for electron, or hole, conduction. Polyfuran is a simple example of this type of π electron-conjugated structure and has been the subject of different works.[5−7] It shows a reasonable electronic conductivity (100 S/cm), which can be compared to maximum conductivities of 500 S/cm for polypyrrole and 2000 S/cm for polythiophene. Polyfuran has a number of other desirable properties, such as flexibility, corrosion resistance, high chemical inertness, and ease of processing.

The furan ring has been the subject of many experimental and theoretical investigations concerning exclusively its molecular structure.[8−15] All of them conclude that the molecule is planar and has C_{2v} symmetry.

A number of previous works are of particular relevance to the present paper. Fourme[13] used X-ray diffraction to reveal a phase transformation at 150 K from a high-temperature disordered phase to a low-temperature ordered phase (phase 2) that belongs to space group $P4_12_12$, with four molecules in the unit cell. Cordell and Boggs[14] revised these previous results, including a comparison between the experimental gas-phase[11]

[†] University of Jaén.
[‡] Interfacultair Reactor Institute.

(1) Sundberg, R. J.; Martin, R. B. *Chem. Rev.* **1974**, *74* (4), 471−517.
(2) Motte-Tollet, F.; Eustatiu, G.; Roy, D. *J. Chem. Phys.* **1996**, *105* (17), 7448−7453.
(3) Hussain, S.; Fawcett, A. H.; Taylor, P. *Prog. Org. Coat.* **2002**, *45* (4), 435−439.
(4) MacDiarmid, A. G. *Synth. Met.* **2002**, *125* (1), 11−22.
(5) Hernández, V.; Ramírez, F. J.; Zotti, G.; López Navarrete, J. T. *J. Chem. Phys.* **1993**, *98* (2), 769−783.
(6) Salzner, U.; Lagowski, J. B.; Pickup, P. G.; Poirier, R. A. *Synth. Met.* **1998**, *96* (3), 177−189.
(7) Saxena, V.; Malhotra, B. D. *Curr. Appl. Phys.* **2003**, *3* (2−3), 293−305.

and crystal structures[13] data and those calculated by theory. There is extensive literature concerning the experimental vibrational spectra of furan.[16−23] The first INS spectrum was reported by Beta et al.,[24] in 2001, for furan adsorbed into zeolites, but they made no attempt to assign the normal modes. In addition, there exist a considerable number of works[25−36] that combined experiment and theory or that were exclusively theoretical at different calculation levels, each aiming at a good description of the vibrational spectrum of the furan molecule. The work of Rico et al.[27] is worthy of mention as it has been regarded as a reference with well-accepted assignments.

As a result of the impressive body of work over the past 50 years, we now have an unambiguous assignment of the vibrational spectrum of the isolated molecule of furan, and the present work extends this to the nature and magnitude of the intermolecular interactions that arise in the solid state and how these affect the vibrational dynamics. This is achieved by using DFT calculations for the monomer, a hydrogen-bonded dimer, and the full periodic crystal structure. By using a topological analysis of the electron density using the atoms in molecules (AIM) theory,[37] we are able to determine the bond paths between a furan molecule and its neighbors in the same orientation as in the crystal structure. A similar analysis of a H-bonded dimer was made using natural bond orbital (NBO) calculations[38] for the monomer and the dimer, with an analysis of the electron charge transfer through the intermolecular contacts. The results of the electron charge-density analysis allow us to relate molecular and physical properties (i.e., the electron conductivity) of furan in polymeric form (i.e., polyfuran) that could be extended to similar systems in which extended π systems give rise to electrical conductivity.

We also use DFT calculations to gauge the relative importance of solid-state effects in the vibrational dynamics of furan. For this, we compare the experimental INS spectrum with calculated spectra in the isolated molecule approach, as in previous studies of other molecular species of the same size,[39−43] and for the crystal, following recent work on similar systems.[44,45] This not only allows a better understanding of the interactions but also provides an experimental validation of the calculated position and curvature of the potential energy in which the nuclei reside. INS spectroscopy is particularly powerful in this respect because the scattering arises from the interaction of neutrons with atomic nuclei, and the observed frequencies and intensities can both be easily compared with calculated values. If required, the whole experimental INS profile can be used for fitting the initial values of the force constants (or of the scale factors) of a molecular force field. This is a considerable advantage compared with the optical spectroscopies, where the spectral profile is often intractable, and the quantitative use of intensities in force-constant or scale-factor refinement is still a difficult proposition.

2. Experimental Section

The sample (from Aldrich, 99%) was wrapped in aluminum foil and loaded into a standard liquid helium cryostat, controlled at $T < 20$ K. The INS spectrum was obtained by using the TFXA spectrometer at the ISIS pulsed neutron source (in the Rutherford Appleton Laboratory, Chilton, U.K.), which has an energy resolution of <2%.

A data acquisition time of 24 h was required to obtain satisfactory counting statistics for the whole spectrum. It is important that the sample be maintained at a low temperature in order to sharpen the vibrational fundamental bands and to decrease the intensity of the phonon wings. Note that the TFXA spectrometer has recently been rebuilt and now has improved resolution and considerably shorter counting times. The new spectrometer is called TOSCA, for which more details can be found at www.rl.ac.uk.

3. Computational Details

Molecular geometry optimization was achieved using GAUSSIAN 98[46] on a Digital Alpha Server 2000. This was performed using Becke's three-parameter exchange functional in conjunction with Lee, Yang, and Parr's correlation functional (B3LYP).[47,48] The standard split-valence basis set, 6-31G*,[49,50] was used at this level because it has been demonstrated that it provides a good compromise between calculation time and quality of the results for the INS spectrum analysis in small heterocyclic systems.[39−43] Vibrational frequencies were calculated from analytic second derivatives to check the minimum on the potential-energy surface. The calculation at this level is in agreement

(8) Schomaker, V.; Pauling, L. *J. Am. Chem. Soc.* **1939**, *61*, 1769−1780.
(9) Sirvetz, M. H. *J. Chem. Phys.* **1951**, *19*, 1609−1610.
(10) Bak, B.; Hansen, L.; Rastrup Andersen, J. *Discuss. Faraday Soc.* **1955**, *19*, 30−39.
(11) Bak, B.; Christensen, D.; Dixon, W. B.; Hansen-Nygaad, L.; Rastrup Andersen, J.; Schottländer, M. *J. Mol. Spectrosc.* **1962**, *9*, 124−129.
(12) Mata, F.; Martin, M. C.; Ole Sorensen, G. *J. Mol. Struct.* **1978**, *48* (2), 157−163.
(13) Fourme, R. *Acta Crystallogr. B* **1972**, *28*, 2984−2991.
(14) Cordell, F. R.; Boggs, J. E. *J. Mol. Struct. (THEOCHEM)* **1988**, *164* (1−2), 175−182.
(15) Liescheski, P. B.; Rankin, D. W. H. *J. Mol. Struct.* **1989**, *196*, 1−19.
(16) Manzoni-Ansidei, R.; Rolla, M. *Atti. Accad. Lincei.* **1938**, *27*, 410−413.
(17) Reitz, A. W. *Z. Phys. Chem.* **1937**, *B38*, 275−291.
(18) Pickett, L. W. *J. Chem. Phys.* **1942**, *10*, 660−663.
(19) Thompson, H. W.; Temple, R. B. *Trans. Faraday Soc.* **1945**, *41*, 27−34.
(20) Bak, B.; Brodersen, S.; Hansen, L. *Acta Chem. Scand.* **1955**, *9*, 749−762.
(21) Rico, M.; Barrachina, M.; Orza, J. M.; Michel, G. *Anal. Fís. Quím.* **1965**, *LXI-A*, 141−170.
(22) Loisel, J.; Pinan-Lucarre, J.-P.; Lorenzelli, V. *J. Mol. Struct.* **1973**, *17* (2), 341−354.
(23) Klots, T. D.; Chirico, R. D.; Steele, W. V. *Spectrochim. Acta, Part A* **1994**, *50* (4), 765−795.
(24) Beta, I. A.; Jobic, H.; Geidel, E.; Böhlig, H.; Hunger, B. *Spectrochim. Acta, Part A* **2001**, *57* (7), 1393−1403.
(25) Orza, J. M.; Rico, M.; Barrachina, M. *J. Mol. Spectrosc.* **1966**, *20* (3), 233−239.
(26) Biarge, J. F.; Orza, J. M.; Rico, M.; Morcillo, J. M. *Anal. Fís. Quím.* **1961**, *LVII-A*, 117−134.
(27) Rico, M.; Barrachina, M.; Orza, J. M. *J. Mol. Spectrosc.* **1967**, *24*, 133−148.
(28) Cyvin, B. N.; Cyvin, S. J. *Acta Chem. Scand.* **1969**, *23*, 3139−3154.
(29) Scott, D. W. *J. Mol. Spectrosc.* **1971**, *37* (1), 77−91.
(30) Bánki, J.; Billes, F.; Grofcsik, A. *Acta Chem. Hung.* **1984**, *116* (3), 283−292.
(31) Simandiras, E. D.; Handy, N. C.; Amos, R. D. *J. Phys. Chem.* **1988**, *92* (7), 1739−1742.
(32) Montero, L. A.; González-Jonte, R.; Díaz, L. A.; Álvarez-Idaboy, J. R. *J. Phys. Chem.* **1994**, *98* (22), 5607−5613.
(33) El-Azhary, A. A.; Hilal, R. H. *Spectrochim. Acta, Part A* **1997**, *53* (9), 1365−1373.
(34) Kwiatkowski, J. S.; Leszczynski, J.; Teca, I. *J. Mol. Struct.* **1997**, *436−437*, 451−480.
(35) Mellouki, A.; Liévin, J.; Herman, M. *Chem. Phys.* **2001**, *271* (3), 239−266.
(36) Billes, F.; Böhlig, H.; Ackermann, M.; Kudra, M. *J. Mol. Struct. (THEOCHEM)* **2004**, *672* (1−3), 1−16.
(37) Bader, R. F. W. *Atoms in Molecules: A Quantum Theory*; Clarendon Press/Oxford Science Publications: Oxford, 1990.
(38) Reed, A. E.; Curtiss, L. A.; Weinhold, F. *Chem. Rev.* **1988**, *88* (6), 899−926.
(39) Navarro, A.; López-González, J. J.; Kearley, G. J.; Tomkinson, J.; Parker, S. F.; Silvia, D. S. *Chem. Phys.* **1995**, *200* (3), 395−403.
(40) Kearley, G. J.; Tomkinson, J.; Navarro, A.; López-González, J. J.; Fernández Gómez, M. *Chem. Phys.* **1997**, *216* (3), 323−335.
(41) Navarro, A.; Fernández Liencres, M. P.; Fernández Gómez, M.; López-González, J. J.; Martínez, E.; Tomkinson, J.; Kearley, G. J. *J. Phys. Chem. A* **1999**, *103* (29), 5833−5840.
(42) Partal, F.; Fernández Gómez, M.; López-González, J. J.; Navarro, A.; Kearley, G. J. *Chem. Phys.* **2000**, *261* (1−2), 239−247.
(43) Navarro, A.; Vázquez, J.; Montejo, M.; López-González, J. J.; Kearley, G. J. *Chem. Phys. Lett.* **2002**, *361* (5−6), 483−491.
(44) Kearley, G. J.; Johnson, M. R.; Plazanet, M.; Suard, E. *J. Chem. Phys.* **2001**, *115* (6), 2614−2620.
(45) Plazanet, M.; Fukushima, N.; Johnson, M. R.; Horsewill, A. J.; Trommsdorff, H. P. *J. Chem. Phys.* **2001**, *115* (7), 3241−3248.

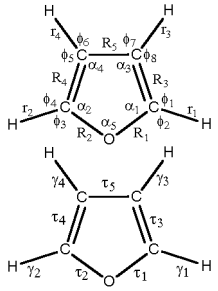

Figure 1. Molecular drawing and internal coordinates for furan.

with previous works,[33,34] showing that the B3LYP method is also more suitable than the HF or MP2 ab initio methods for the vibrational analysis of furan.

The topological analysis of the electronic charge density was performed by using the atoms in molecules methodology (AIM), with the AIM2000 program package.[51] The natural bond orbital calculation was performed using the NBO 4.0 program,[52] as implemented in the Gaussian 98 package.

The CLIMAX[53] program was used to calculate the INS spectral profile from the vibrational frequencies, the atomic displacements resulting from the various ab initio calculations, and the force-constant (or scalar) refinement procedures. For the isolated approximation, the force constants in Cartesian coordinates from the ab initio calculations were used to construct a force field in independent symmetry coordinates.[54] According to the C_{2v} point symmetry for the isolated molecule of furan, such a set of nonredundant symmetry coordinates was obtained by diagonalization of BB^t and by application of the Schmidt orthogonalization procedure.[55] The internal coordinates used in this work are illustrated on the molecular diagram in Figure 1, and the set of independent symmetry coordinates is available as Supporting Information (Table 1S of the Supporting Information). The block-diagonal force-constant matrix was refined by using CLIMAX, which produces $S(Q,\omega)$ intensities, taking full account of the Debye−Waller factor for the fundamentals, overtones, and combinations. All frequencies and atomic displacements were calculated from the force-constant matrix using the GF−Wilson method,[56] without anharmonic corrections. The INS spectral intensities are calculated according to the theory given by Tomkinson et al.[57,58]

Table 1. DFT Optimized Geometry for Furan Compared with Available X-ray Diffraction and Microwave Data in Literature (bond lengths in angstroms and angles in degrees)[a]

	B3LYP/6-31G*	microwave[b]	X-ray[c]
C−H_α	1.081	1.075	
C−H_β	1.079	1.077	
C═C	1.361	1.361	1.322
C−C	1.435	1.431	1.428
C−O	1.364	1.362	1.368
COC	106.7	106.33	106.17
OCC	110.5	110.41	110.14
CCC	106.1	106.3	106.76
OCH	115.6	115.55	
CCH	127.4	127.57	
a			5.69
b			5.69
c			11.92

[a] H_α is the H in the ortho position with respect to the O atom, and H_β is the H in the meta position. [b] From ref 11. [c] From ref 13.

For the periodic DFT calculations, the Cerius2 implementation[59] of DMol3,[60] which uses localized numerical atomic orbitals, was employed. Default settings, as proposed by the Cerius2 implementation, were used with a DND double numerical basis set with polarization functions for carbon. The vibrational spectra for the minimized structure were calculated in the harmonic approximation by using the direct method to obtain the forces. CLIMAX was then used to calculate the neutron spectral profile. In the case of a periodic calculation, this procedure provides the vibrational frequencies corresponding to the Γ point (long wavelength limit), and in the presence of dispersion, there may be some apparent differences between the observed and calculated INS spectral profiles.

4. Results and Discussion

4.1. Structural Analysis. 4.1.1. Optimized Geometry. The energy-minimized molecular geometry for the isolated furan molecule, calculated at the B3LYP/6-31G* level, is given in Table 1, from which it can be seen that the experimental[11,13] and theoretical results are in reasonable agreement. This minimized structure was used as the starting point for calculating the normal modes and molecular force fields. The difference between calculated and experimental values of the C═C distance is larger than those for the other geometric parameters, but as explained in ref 14, this greater difference may be due to an experimental artifact in the X-ray diffraction spectrum analysis.[13] It is probable that the calculated value is more reliable than the experimental value.

A DFT calculation using a single unit cell with periodic boundary conditions was also carried out. The starting point for this calculation was the solid-state structure determined by Fourme,[13] which was later revised by Cordell and Boggs.[14] To avoid negative eigenvalues, this structure was energy minimized, with the cell constants constrained to the experimental values. The resulting structure was only slightly different from that determined crystallographically, with the molecular geometry in the crystal also being given in Table 1.

In ref 13, the authors point out that in the crystal, there are van der Waals contacts between the hydrogen atoms of one molecule and the oxygen (2.50 Å) and carbon (2.70 Å) atoms of the neighboring molecule. These could also be considered to be rather weak hydrogen bonds that would have no meaning

(46) Frish, M.; Trucks, G. W.; Schlegel, H. B.; Scuseria, G. E.; Robb, M. A.; Cheeseman, J. R.; Zakrzewski, V. G.; Montgomery, J. A.; Stratmann, R. E.; Burant, J. C.; Dapprich, S.; Millam, J. M.; Daniels, A. D.; Kudin, K. N.; Strain, M. C.; Farkas, O.; Tomasi, J.; Barone, V.; Cossi, M.; Cammi, R.; Mennucci, B.; Pomelli, C.; Adamo, C.; Clifford, S.; Ochterski, J.; Peterson, G. A.; Ayala, P. Y.; Cui, Q.; Morokuma, K.; Malick, D. K.; Rabuck, A. D.; Raghavachari, K.; Foresman, J. B.; Cioslowski, J.; Ortiz, J. V.; Baboul, A. G.; Stefanov, B. B.; Liu, G.; Liashenko, A.; Piskorz, P.; Komaromi, I.; Gomperts, R.; Martin, R. L.; Fox, D. J.; Keith, T.; Al-Laham, M. A.; Peng, C. Y.; Nanayakkara, A.; Gonzalez, C.; Challacombe, M.; Gill, P. M. W.; Johnson, B.; Chen, W.; Wong, M. W.; Andres, L.; Head-Gordon, M.; Replogle, E. S.; Pople, J. A. *Gaussian 98*, revision A.7; Gaussian, Inc.: Pittsburgh, PA, 1998.
(47) Lee, C.; Yang, W.; Parr, R. G. *Phys. Rev. B* **1988**, *37* (2), 785−789.
(48) Becke, A. D. *J. Chem. Phys.* **1993**, *98* (7), 5648−5652.
(49) Hariharan, P. C.; Pople, J. A. *Theor. Chim. Acta* **1973**, *28* (3), 213−222.
(50) Pople, J. A.; Schlegel, H. B.; Krishman, R.; Defrees, D. J.; Binkley, J. S.; Frisch, M. J.; Whiteside, R. A.; Hout, R. F.; Hehre, W. J. *Int. J. Quantum Chem.* **1981**, *15*, 269−278.
(51) Biegler-König, F.; Schönbohm, J.; Bayles, D. AIM2000: A Program to Analyze and Visualize Atoms in Molecules. *J. Comput. Chem.* **2001**, *22*, 545−559.
(52) Gledening, E. D.; Badenhoop, J. K.; Reed, A. D.; Carpenter, J. E.; Weinhold, F. F. *NBO 4.0*; Theoretical Chemistry Institute, University of Wisconsin: Madison, WI, 1996.
(53) Kearley, G. J. *J. Chem. Soc., Faraday Trans. 2* **1986**, *82* (1), 41−48.
(54) Martínez-Torres, E.; López-González, J. J.; Fernández Gómez, M. *J. Chem. Phys.* **1999**, *110* (7), 3302−3308.
(55) Zerbi, G.; Barnes, A. J.; Orville-Thomas, M. J. *Vibrational Spectroscopy: Modern Trends*; Elsevier: Amsterdam, 1977.
(56) Wilson, E. B., Jr.; Decius, J. C.; Cross, P. C. *Molecular Vibrations*; McGraw-Hill: New York, 1955.
(57) Howard, J.; Boland, C. B.; Tomkinson, J. *Chem. Phys.* **1983**, *77* (1), 145−151.
(58) Tomkinson, J.; Warner, M.; Taylor, A. D. *Mol. Phys.* **1984**, *51* (2), 381−392.
(59) *Cerius2*. BIOSYM/Molecular Simulations: San Diego, CA, 1996.
(60) Delley, B. *J. Chem. Phys.* **1990**, *92* (1), 508−517.

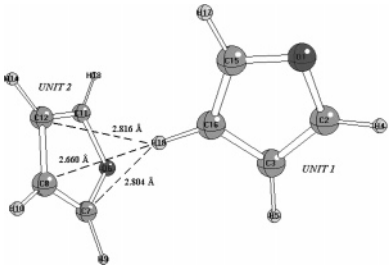

Figure 2. Hydrogen-bond contacts for the H-bonded dimer in solid furan.

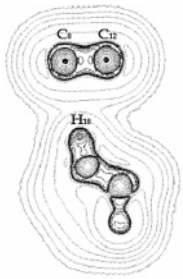

Figure 3. Laplacian contour map showing the critical point associated with the bond path between the C(8) and H(18) atoms. Solid contours are associated with negative and dot contours with positive values of Laplacian.

in the isolated molecule calculation. Because there are experimentally determined hydrogen atom positions, these are determined by the DFT energy minimization. This allows us to analyze the solid-state structure of furan with a combination of a topological analysis of the charge electron density and a NBO calculation for a dimer formed by two of the four molecules existing in the unit cell of furan at low temperature. For convenience we denote this as a "H-bonded dimer".

4.1.2. Topological Analysis for the H-Bonded Dimer. The atoms in molecules theory[37] has been widely applied to many chemical problems because it is particularly useful for investigating the influence of the crystal environment and intermolecular interactions. Both inter- and intramolecular interactions have been analyzed by using Bader's topological analysis of the charge electron density, $\rho(r)$. The localization of the critical points (CP) in the $\rho(r)$ and the arrangement and the values of its Laplacian at these points have shown to be very suitable tools for the characterization of molecular electronic structure in terms of the nature and magnitude of the interactions. The CPs (i.e., points of the charge electron distribution where $\nabla\rho(r) = 0$) are classified by analyzing the Hessian matrix of $\rho(r)$. The CPs that have three nonzero eigenvalues (i.e., two negative and one positive) correspond to bond critical points (BCP) (3, −1). We analyze only these CPs in the present study. The sign of the Laplacian, $\nabla^2\rho(r)$, at these points indicates that the charge electron density is either locally depleted [$\nabla^2\rho(r) > 0$] or locally concentrated [$\nabla^2\rho(r) < 0$]. This relationship is very useful for classifying interactions. Thus, $\nabla^2\rho(r) > 0$ results are associated with closed-shell interactions, such as those that occur for hydrogen bonds in which $\rho(r)$ should be small.

The existence of bond paths between the furan rings in the crystal and the (3, −1) BCPs were examined using the AIM2000[59] program, using the charge density calculated for the optimized geometry of the periodic crystal. In the first instance, we focus our attention on the H-bonded dimer of furan described above. The H-bond contacts between both furan rings are shown in Figure 2. Inspection revealed a bond path and its corresponding (3, −1) BCP between H_{18} and C_8. (A figure showing the bond path is available as Supporting Information.) This bond path goes from the H_{18} to the C_8-C_7 bond and then bends sharply toward the C_8 atom. Therefore, we propose that the $C_{16}-H_{18}\cdots C_8$ contact should be classified as a $C-H\cdots\pi$ interaction. Figure 3 illustrates the contour map of the Laplacian of $\rho(r)$ for the dimer in the plane defined by the atoms H_{18}, C_8, and C_{12} and shows that the shape between H_{18} and C_8 resembles that of a saddle. The Laplacian is positive between these two atoms, and along the direction of the interaction, it has a minimum at the critical point (the CP is not necessary on the same plane of the figure). According to the nature of the interaction, at this CP, the Laplacian takes a positive value (0.0269 au), and thus at that point, there is a small electron density (0.0087 au). The hydrogen-bond interactions extend over the crystal, and thus the CP (3, −1) associated with the $C-H\cdots\pi$ interaction between the two molecules of the H-bonded dimer exists between all pairs of furan rings in the solid state.

It is likely that a similar intermolecular H-bond interaction exists in polyfuran either between end groups or between end groups and other points on the conjugated system. Such interactions would play an important role in charge transfer between neighboring polymer chains. We can obtain an estimate for the charge-transfer integral, b[61]

$$b \approx \frac{1}{2}\sqrt{(E_{D1} - E_{D2})^2 - (E_1 - E_2)^2}$$

where E_{D1} and E_{D2} are the energies of the HOMO and HOMO-1 levels in the dimer, respectively, and E_1 and E_2 are the corresponding energies for the furan units separated by infinity. This yields a value of 0.168 eV, compared with 2.329 eV for two furan units in a polyfuran chain. If we assume that the charge-transfer integral varies as the cosine of the intermonomer angle between two furan units in the polymer, we find that the charge-transfer integral for the H-bonded dimer is the same as for a "kink" in the polymer, with an intermonomer angle of 85°. Such kinks are present when polymers crystallize and where the connectivity of the long chain molecules usually hinders the formation of perfect crystals and leads to semicrystalline materials.

4.1.3. NBO Calculation for the H-Bonded Dimer. The NBO[38] analysis is used to identify and confirm the possible intermolecular interactions between the units that would form the H-bonded furan dimer, as detected via the topological analysis. In the NBO analysis, the electronic wave function is interpreted as a set of occupied Lewis-type orbitals, paired with a set of formally unoccupied non-Lewis-type orbitals. The electronic interactions within these orbitals, the deviations from the Lewis electronic structure, and the delocalization effects can be interpreted as charge transfer between the filled Lewis orbitals (donors) and the theoretically empty non-Lewis orbitals (acceptors).[38] The magnitude of these delocalization effects can be determined from an analysis of the off-diagonal elements in the Fock matrix in the NBO basis by taking account of all possible donor−acceptor interactions and then by calculating the strength of them all by second-order perturbation theory.

The H-bonded dimer structure has been taken from the optimization of the solid structure, as described above. The NBO method calculates different charges for each furan unit in the

(61) Newton, M. D. *Chem. Rev.* **1991**, *91* (3), 767−792.

Table 2. NBO Analysis of the Furan Monomer and Dimer: Occupation Numbers for the σ^*_{CH} Antibonds and the π_{CC} Bonds, with Their Respective Energies

		occupancy	energy (au)
monomer	$\pi_{C2,4-C3,5}$	1.8830	−0.2630
	$\sigma^*_{C-H\alpha}$ [a]	0.0141	0.4857
	$\sigma^*_{C-H\beta}$ [b]	0.0117	0.4885
dimer unit 1 (acceptor)	π_{C2-C3}	1.8799	−0.2564
	$\pi_{C15-C16}$	1.8768	−0.2543
	$\sigma^*_{C2-H4\ (\alpha)}$	0.0146	0.4670
	$\sigma^*_{C5-H17\ (\alpha)}$	0.0145	0.4675
	$\sigma^*_{C3-H5\ (\beta)}$	0.0124	0.4680
	$\sigma^*_{C16-H18\ (\beta)}$	0.0159	0.4938
dimer unit 2 (donor)	π_{C7-C8}	1.8773	−0.2689
	$\pi_{C11-C12}$	1.8757	−0.2674
	$\sigma^*_{C7-H9\ (\alpha)}$	0.0144	0.4585
	$\sigma^*_{C11-H13\ (\alpha)}$	0.0142	0.4603
	$\sigma^*_{C8-H10\ (\beta)}$	0.0123	0.4596
	$\sigma^*_{C12-H14\ (\beta)}$	0.0122	0.4596

[a] H_α is the hydrogen linked to C atoms in the ortho position with respect to the oxygen. [b] H_β is the hydrogen linked to C atoms in the meta position with respect to the oxygen.

H-bonded dimer. One of them, unit 2, presents a slightly positive charge, while the other, unit 1, bears an equivalent negative charge, −0.0055 au. Clearly, unit 1 acts as a charge acceptor, whereas unit 2 is a charge donor. The analysis of the off-diagonal elements of the Fock matrix by second-order perturbation theory shows two interactions between both units as charge transfers from the π-bonding orbitals in unit 2 to the antibonding $\sigma^*_{C16-H18}$ orbital in unit 1, which is defined as $\pi_{C7-C8} \rightarrow \sigma^*_{C16-H18}$ and $\pi_{C11-C12} \rightarrow \sigma^*_{C16-H18}$. The magnitudes of these interactions are 1.33 and 0.23 kcal/mol, respectively, from which it can be seen that a $\pi_{C-C} \rightarrow \sigma^*_{C-H}$ interaction between unit 1 and unit 2 is stronger when the C_8 atom is also involved, which is reasonable taking into account that the bond path was found to involve C_8 and C_{18}.

In Table 2, the results of the NBO calculation for the area in question are given. The electronic population in the antibonding $C_{16}H_{18}$ orbital of unit 1, $\sigma^*_{C16-H18}$, increases to 0.0159 au with respect to its value in the monomer, 0.0117 au, and is even higher than that of the $C_{12}H_{14}$ bond placed in unit 2 (donor), 0.0122 au. The remaining antibonding CH occupancies in the dimer change less with respect to the monomer. Similar conclusions can be obtained if we take into account the analysis of the energy of each orbital. As mentioned above, $\sigma^*_{C16-H18}$ is the orbital that is more destabilized in the dimer. We also find that the $C_{16}H_{18}$ bond length for the dimer is longer than the C−H(β) bond length in the monomer: 1.096 and 1.081 Å, respectively. It can also be seen in Table 2 that the π orbital population tends to be lower in both units of the dimer, compared with the value obtained for the monomer, with the largest decrease being for the donor, unit 2.

These results are in excellent agreement with the topological analysis of the previous section that showed a bond path between C_8 and H_{18}, and they demonstrate the presence of bonding or association between all pairs of furan molecules in the solid material.

4.1.4. Topological Analysis for the Eight-Monomer Cluster. The dimer model does not embody the local symmetry of each furan molecule, and it is interesting to enquire if the topological analysis of electron density is significantly different for a more realistic cluster model. For this determination, we

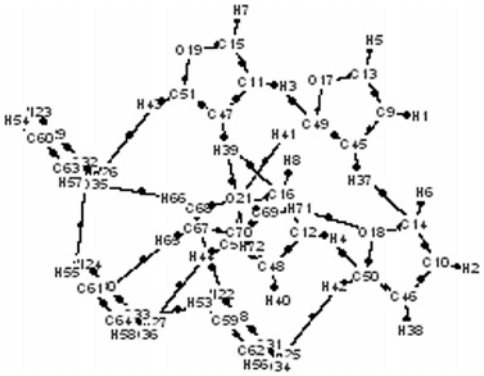

Figure 4. Eight monomer clusters in solid furan showing the BCP.

Table 3. BCPs Found in the Eight-Monomer Furan Cluster

interaction	ρ(r)(au)	$\nabla^2\rho$(r) (au)	C–H distance (Å)	H···C distance (Å)
$C_{11}-H_3\cdots C_{49}$	0.0016	0.0055	1.096	3.492
$C_{12}-H_4\cdots C_{50}$	0.0016	0.0055		
$C_{45}-H_{37}\cdots C_{14}$	0.0016	0.0056		
$C_{47}-H_{39}\cdots C_{16}$	0.0016	0.0056		
$C_{61}-H_{55}\cdots C_{32}$	0.0016	0.0055		
$C_{28}-H_{22}\cdots C_{64}$	0.0016	0.0056		
$C_{70}-H_{72}\cdots C_{48}$		0.0270	1.096	2.660
$C_{47}-H_{39}\cdots C_{70}$	0.0086	0.0268		
$C_{61}-H_{55}\cdots C_{30}$	0.0088	0.0270		
$C_{28}-H_{22}\cdots C_{67}$	0.0086	0.0268		
			C–H distance (Å)	H···O distance (Å)
$O_{18}\cdots H_{71}-C_{69}$	0.0087	0.0309	1.092	2.484
$O_{21}\cdots H_{41}-C_{49}$	0.0087	0.0308		
$O_{35}\cdots H_{66}-C_{68}$	0.0088	0.0309		
			C–H distance (Å)	H···H distance (Å)
$C_{33}-H_{27}\cdots H_{44}-C_{52}$	0.0013	0.0044	1.092	3.026
$C_{31}-H_{25}\cdots H_{42}-C_{50}$	0.0013	0.0044		
$C_{32}-H_{26}\cdots H_{43}-C_{51}$	0.0013	0.0044		

constructed a cluster containing eight furan molecules such that the central molecule has exactly the same environment and local symmetry as in the crystal (Figure 4). The application of the AIM method to the cluster yields a total of 16 BCPs, which are listed in Table 3. The C−H bond lengths in the cluster have been also included in order to compare them with the C−H bond lengths in the isolated molecule. In all of the cases, this distance increases when the hydrogen bond is formed, as compared with the C−H bond distance in the molecular calculation and microwave data.

As can be seen in Figure 4, 13 intermolecular contacts are C−H···π, and the interaction of $C_{70}-H_{72}\cdots C_{48}$ is virtually the same as that found for the dimer, with the values for the density and Laplacian being 0.0087 and 0.0270 au, respectively (the values for the isolated dimer were 0.0087 au for density and 0.0269 au for Laplacian). In the cluster, three C−H···π interactions were found: $C_{47}-H_{39}\cdots C_{70}$, $C_{61}-H_{55}\cdots C_{30}$, and $C_{28}-H_{22}\cdots C_{67}$, with similar strength to the former. Three new C−H···O interactions were found: $O_{18}\cdots H_{71}-C_{69}$, $O_{21}...H_{41}-C_{49}$, and $O_{35}...H_{66}-C_{68}$, with values for the density, 0.0087(8) and 0.0309(8) au for Laplacian, almost identical to those for C−H···π interactions.

Finally, three H···H interactions were found where a bond path links a pair of similar hydrogen atoms. It has been

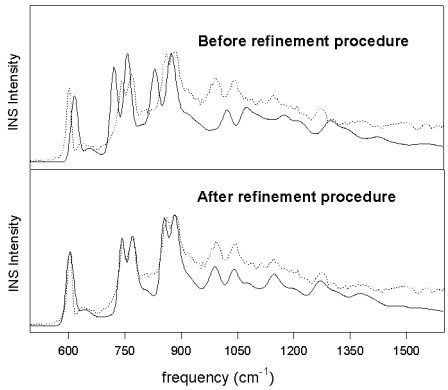

Figure 5. Observed (dotted) and calculated (continuous) spectra for furan at the B3LYP/6-31G* level, before and after the refinement procedure.

demonstrated that despite the weakness of these interactions, compared with that of the C−H···π and C−H···O interactions, the H···H interactions do indeed reduce the total energy.[62]

All of these intermolecular contacts play a role in the mechanism of crystallization determining the final structure in the solid furan, and these contacts could also be present in the crystal growing of polyfuran chains. Furthermore, the corresponding charge-transfer integrals for all of the interactions could contribute to the final conducting properties in conjugated polymers, as it is in the case of polyfuran.

4.2.Vibrational Analysis. So far, the only validation of the DFT calculations is that they reproduce the measured crystal structure satisfactorily, and to obtain better confirmation of the H-bonding interactions, we have made a vibrational analysis of the isolated molecules and the full periodic structure. The relative importance of solid-state effects can be assessed by comparing these with the measured vibrational dynamics. We take this opportunity to make a rather complete vibrational analysis.

Figure 5 shows the calculated INS spectrum of an isolated furan molecule by using the theoretical molecular force field at the B3LYP/6-31G* level (before refinement). The difference between the observed and calculated spectra is within the range expected for this sort of work.[39−43] The goal now is to determine whether the spectral differences can be significantly reduced by refining the initial force field and whether this provides a meaningful final force field. Because we use the whole INS spectral profile for our refinement, we would normally expect that any attempt to "refine in" solid-state effects would not lead to a simultaneous improvement in both frequency and intensity agreement. Clearly, a refinement based on frequency data alone is a more hazardous proposition. The intensity constraint provided by the profile fitting procedure ensures that a reasonable description of the atomic displacements (hence assignments) is obtained. Errors in the model, such as the neglect of intermolecular interactions, can be gauged from the spectral agreement.

Our assignments, based on the above procedure, confirm those proposed by Rico[27] for the IR spectrum. With the INS spectrometer used in the present work, the energy transfer and the momentum transfer are strongly coupled, and consequently, the quality of the spectrum above 2000 cm^{-1} is rather poor. Under these circumstances, we use the frequency data from IR or Raman spectra as a constraint for the C−H stretching modes, $\sim$3000cm^{-1}, in the refinement of the INS profile in this spectral region. This is not a serious concern because the principal area of conflict in the assignment of the spectra in the literature has been in the region between 800 and 900 cm^{-1}, in particular, for the assignment of the out-of-plane mode, ν_9. In this spectral region, the INS spectra are of good quality, and as can be seen in Figure 5, two peaks are well resolved at 854 cm^{-1}, assigned to ν_{12}, and at 880 cm^{-1}, which arises from the out-of-plane mode, ν_9, and two in-plane modes, ν_8 and ν_{21}. Table 4 gives the relative INS intensities for all normal modes after the refinement of the force field, and it is clear that the calculated intensity of ν_8 and ν_{21} is much less than that for ν_9. Therefore, the intensity observed at 880 cm^{-1} principally arises from the

Table 4. Observed IR and Raman, Observed INS and Refined Frequencies (isolated molecule force field, in cm^{-1}) for Furan, as Well as INS Relative Intensity and Spectral Assignment

mode		observed IR and Raman[27]	observed INS	refined	INS relative intensity	description[d]
A_1	ν_1	3167	3167[b]	3167	0.182	$\nu_{C-H\alpha}$[e] + $\nu_{C-H\beta}$[f]
	ν_2	3140	3140[b]	3139	0.180	$\nu_{C-H\beta} + \nu_{C-H\alpha}$
	ν_3	1491	1485	1485	0.115	$\nu_{C=C} + \delta_{HCO}$
	ν_4	1384	1372	1372	0.372	$\nu_{C-C} + \delta_{ring} + \delta_{HCO} + \delta_{HCC}$
	ν_5	1140	1146	1146	0.582	$\nu_{C=C} + \delta_{HCO} + \delta_{HCC}$
	ν_6	1066	1074	1075	0.190	$\nu_{C-O} + \nu_{C-C} + \delta_{ring}$
	ν_7	995	992	991	0.537	$\nu_{C-O} + \nu_{C-C} + \delta_{ring} + \delta_{HCC}$
	ν_8	871	886[c]	886	0.170	δ_{ring}
A_2	ν_9	863[a]	880	880	0.809	$\gamma_{C-H\beta} + \tau_{ring}$
	ν_{10}	728	742	742	0.810	$\gamma_{C-H\alpha} + \tau_{ring}$
	ν_{11}	613	605	605	0.587	τ_{ring}
B_1	ν_{12}	838	854	854	0.981	$\gamma_{C-H\alpha} + \gamma_{C-H\beta} + \tau_{ring}$
	ν_{13}	745	769	769	1.000	$\gamma_{C-H\alpha} + \gamma_{C-H\beta} + \tau_{ring}$
	ν_{14}	603	602	602	0.189	τ_{ring}
B_2	ν_{15}	3161	3161[b]	3161	0.187	$\nu_{C-H\alpha} + \nu_{C-H\beta}$
	ν_{16}	3129	3129[b]	3129	0.180	$\nu_{C-H\beta} + \nu_{C-H\alpha}$
	ν_{17}	1556	1553	1553	0.106	$\nu_{C=C} + \delta_{ring} + \delta_{HCC}$
	ν_{18}	1267	1272	1272	0.670	$\delta_{HCO} + \delta_{HCC}$
	ν_{19}	1180	1211	1211	0.235	$\nu_{C-O} + \nu_{C-C} + \delta_{ring} + \delta_{HCC}$
	ν_{20}	1040	1042	1042	0.611	$\nu_{C-O} + \nu_{C-C} + \delta_{ring} + \delta_{HCC} + \delta_{HCO}$
	ν_{21}	873	891[c]	891	0.109	δ_{ring}

[a] Nonobserved (see ref 27). [b] From ref 27. [c] Theoretical values. [d] Abbreviations used: ν, stretching; δ, angle deformation; γ, wagging; τ, torsion. [e] H_α is the hydrogen linked to C atoms in the ortho position with respect to the oxygen. [f] H_β is the hydrogen linked to C atoms in the meta position with respect to the oxygen.

Table 5. Comparison between Vibrational Frequencies (cm^{-1}) and Relative INS Intensities from Both Molecular and Periodic DFT Calculations

		Molecular		Periodic				Molecular		Periodic	
mode	symmetry	frequency (cm^{-1})	INS relative intensity	frequency (cm^{-1})	INS relative intensity	mode	symmetry	frequency (cm^{-1})	INS relative intensity	frequency (cm^{-1})	INS relative intensity
				3169	0.018					1038	0.502
ν_1	A_1	3307	0.160	3169	0.018	ν_{20}	B_2	1073	0.589	1027	0.526
				3169	0.018					1027	0.526
				3168	0.018					1020	0.546
				3163	0.019					988	0.598
ν_{15}	B_2	3302	0.161	3163	0.019	ν_8	A_1	1024	0.680	982	0.589
				3163	0.019					982	0.589
				3163	0.019					976	0.573
				3121	0.018					875	0.493
ν_2	A_1	3275	0.174	3121	0.018	ν_{21}	B_2	891	0.104	873	0.267
				3121	0.018					873	0.267
				3120	0.019					870	0.205
				3113	0.019					867	0.118
ν_{16}	B_2	3264	0.177	3112	0.019	ν_8	A_1	886	0.161	867	0.462
				3112	0.019					866	0.199
				3111	0.019					866	0.199
				1554	0.051					864	0.152
ν_{17}	B_2	1614	0.099	1551	0.051	ν_9	A_2	873	0.887	863	0.624
				1551	0.051					863	0.624
				1548	0.050					854	0.768
				1482	0.073					842	0.816
ν_3	A_1	1529	0.162	1476	0.070	ν_{12}	B_1	831	0.944	833	0.829
				1476	0.070					833	0.829
				1473	0.069					821	0.836
				1390	0.116					749	1.000
ν_4	A_1	1433	0.208	1386	0.117	ν_{13}	B_1	758	1.000	749	1.000
				1386	0.117					745	0.976
				1383	0.118					738	0.964
				1235	0.415					719	0.964
ν_{18}	B_2	1299	0.648	1235	0.415	ν_{10}	A_2	723	0.958	717	0.970
				1234	0.417					715	0.960
				1233	0.403					715	0.960
				1188	0.142					622	0.321
ν_{19}	B_2	1223	0.273	1188	0.142	ν_{14}	B_1	623	0.279	622	0.321
				1186	0.151					621	0.364
				1184	0.144					614	0.444
				1143	0.274					606	0.394
ν_5	A_1	1176	0.483	1140	0.228	ν_{11}	A_2	614	0.365	602	0.450
				1140	0.228					602	0.450
				1138	0.207					601	0.453
				1091	0.253						
ν_6	A_1	1100	0.277	1072	0.323						
				1072	0.323						
				1058	0.361						

out-of-plane mode, ν_9, which is mainly a C−H wagging. Due to their low intensities in the INS spectrum, the in-plane modes, ν_8 and ν_{21}, have been assigned at their calculated frequencies.

We obtain the initial force-constant matrix in terms of symmetry coordinates by making the appropriate transformation of the matrix obtained from the ab initio calculations. In the A_1 and B_2 blocks, we fitted all diagonal and, in the case of A_1, two off-diagonal force constants to reproduce the frequencies and intensities of the in-plane modes. The A_2 and B_1 blocks correspond to out-of-plane modes, and in this case, we minimized the differences between observed and calculated spectra by refining all of the diagonal and nonzero off-diagonal force constants. Observed INS and IR−Raman frequencies, INS relative intensities, and the description of each vibrational normal mode are collected in Table 4.

The spectrum before and after the refinement is shown in Figure 5, and it can be seen that the refinement procedure leads to a considerable improvement. It is interesting to note that above 1000 cm^{-1}, the observed intensity is rather higher than that calculated particularly between 1000 and 1200 cm^{-1}. While it is known that the validity of the partial recoil approximation for phonon wings decreases with increasing energy (momentum) transfer, it normally leads to a far more progressive decrease in the apparent background of the calculated spectrum. This manifests itself as an increasing separation between observed and calculated profiles with increasing energy transfer.

The isolated molecule calculation provides a reasonable starting model with force constants that can be refined to provide acceptable agreement between observed and calculated INS spectral profiles. Nevertheless, while the final frequency agreement is rather pleasing, the general trend of calculated spectral intensity after refinement is noticeably too strong at low energies

(62) Matta, C. F.; Hernández-Trujillo, J.; Tang, T.; Bader, R. *Chem.—Eur. J.* **2003**, *9*, 1940−1951.

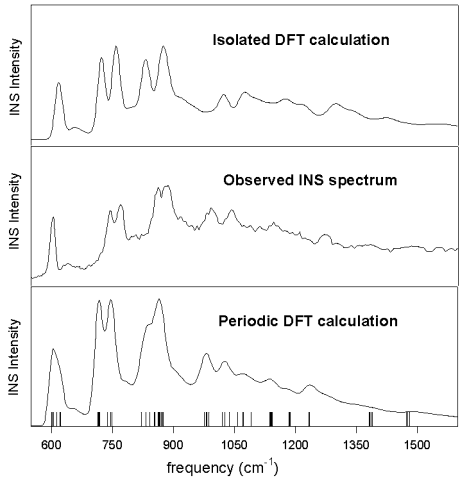

Figure 6. Comparison of the experimental INS spectrum of solid furan with DFT calculated spectra for the isolated molecule and the crystal.

and too weak at high energies. This trend could not be removed by adjustment of the external Debye−Waller factor, which we had refined to a rather reasonable value of 0.02 Å^2. This result is comforting since if we could refine the errors away, the procedure would be of limited value.

Clearly, the question is whether we can obtain a better result by using a periodic model, and if so, can the improvement be attributed to the intermolecular H-bonding? We performed a periodic DFT calculation using a single unit cell with periodic boundary conditions. The energy of the system was minimized with the unit-cell parameters being constrained to their experimental values. This resulted in only small changes to atomic positions. This model takes into account the intermolecular interactions, but because we calculate the derivatives of the energy periodically, the vibrations among all unit cells will be in-phase. This corresponds to the long wavelength limit, which is appropriate for optical spectroscopies, but it could lead to problems for the INS spectrum in the case of dispersion. However, in the present case, this is not expected for modes above 200 cm^{-1} because there are no strong (H-bonding) interactions in this system.[63]

The results of the normal mode calculation for furan, based on total-energy calculations from periodic DFT, are collected in Table 5 together with those obtained for the isolated molecule, also from DFT calculations. It can be seen there that the frequencies from the periodic calculation are systematically lower than the values for the isolated molecule approximation. For the periodic calculation, each normal mode is calculated as a quadruplet due to coupling between the four furan molecules in the unit cell. With a few exceptions, the calculated splitting (factor group splitting) is rather small. This tends to support our supposition above that dispersion should not be a problem.

In Figure 6, we compare the 550−1600 cm^{-1} spectral region for the experimental and calculated INS spectra from both the isolated molecule approach (without refinement) and the periodic model. The bars at the bottom of the figure show the peak positions calculated for the periodic model. It is clear that the periodic model provides much better overall agreement in this region and virtually eliminates the need to refine force constants. The region above 1000 cm^{-1} is improved, and while the isolated molecule calculation predicts a large splitting in the 800−900 cm^{-1} region, the periodic calculation predicts a smaller splitting, which is in better agreement with the experimental profile. The only real exception is around 600 cm^{-1}, where the spectrum is better reproduced by the isolated furan molecule model. In this region, the isolated model predicts a difference of 9 cm^{-1} between ν_{11} and ν_{14}, while the periodic calculation predicts a difference of 21 cm^{-1}. This result produces a shoulder close to the main peak at 605 cm^{-1} of the calculated spectrum from the periodic model that is not observed in the experimental spectrum.

Both isolated molecule and periodic calculations predict slightly too much intensity for the INS spectral bands of the ν_{10} and ν_{13} modes of furan in the 740−770 cm^{-1} region, both of which are associated with C−H (α and β) waggings. While DFT cannot be expected to give perfect results, this intensity difference could arise from dispersion, which is not always obvious in the peak shape. In this event, it would be reasonable to attribute the dispersion to H-bonding interactions. Indeed, inspection of Table 5 reveals significant factor group splitting for several modes below 850 cm^{-1}, which is also indicative of intermolecular interaction.

5. Conclusions

Intermolecular contacts between rings of furan in the solid state have been interpreted by a topological analysis of the theoretical electron density and by an NBO calculation. The present work reveals the existence of C−H···π, C−H···O, and H···H intermolecular contacts between adjacent molecules in solid furan. These results could be extrapolated to the polyfuran, suggesting possible interactions between end groups of the polymer chains that could affect its conducting properties. Similarly, these conclusions could be extended to other conjugated polymers in which charge transfer between chains could play an important role in the macroscopic conductivity.

A detailed analysis of the vibrational spectrum validates the model and the DFT calculations and further provides a consistent picture of how these H-bonding interactions modify the molecular vibrations in the solid state. These calculations, combined with the experimental INS spectra, provide complete an up-to-date description of the normal modes for the furan molecule.

Some caution should be exercised for DFT calculations using the isolated molecule approach. Provided that adequate data are available, the consequences of solid-state effects can be assessed, and in the present work, this becomes apparent through the difficulties experienced in reproducing the measured spectral profile. In fact, furan is an intermediate case in which the isolated molecule approximation certainly provides the basis for an unambiguous assignment, but the details of the eigenvectors will not be correct. Where intermolecular interactions are strong, the isolated molecule approach can provide eigenvectors that are not even approximately correct, as shown by ref 44.

Solid-state effects are made evident by taking the periodicity of the crystals into account, and if these are significant, then the periodic calculation will provide better agreement with the observed INS spectrum. The aim of the present study is to understand the most important intermolecular interactions and how these may relate to charge transfer between polymer chains. This we have established, and the residual differences between

(63) van Eijck, L.; Johnson, M. R.; Kearley, G. J. *J. Phys Chem. A* **2003**, *107* (42), 8980−8984.

observed and calculated spectra could certainly be further reduced in two ways. First, a neutron diffraction study of the low-temperature phase (at 20 K) would provide a better starting model. Second, the effects of dispersion could be achieved by using a lattice dynamics calculation.[64] However, both of these extensions go beyond the aim of the present study.

Acknowledgment. We are grateful to ISIS for enabling us to record the INS spectrum, and the European Community for providing financial support. M.M. thanks Fundación Ramón Areces for a Ph.D. grant, supporting this work. The authors thank Dr. Francisco Partal for helpful discussions.

(64) Schimmel, H. G.; Johnson, M. R.; Kearley, G. J.; Ramirez-Cuesta, A. J.; Huot, J.; Mulder, F. M. *J. Mater. Sci. Eng B* **2004**, *108*, 38−41.

Supporting Information Available: Tables 1S−3S and Figure 1S. Table 2S includes the more significant terms of the potential-energy distribution (PED) and the calculated B3LYP/6-31G* modes. Initial and final values of the force constants are collected in Table 3S. This material is available free of charge via the Internet at http://pubs.acs.org.

JA040130Y